

Hierarchy Influenced Differential Evolution: A Motor Operation Inspired Approach

Keywords: Differential Evolution, Metaheuristics, Continuous Optimization, Hierarchical Influence

Abstract: Operational maturity of biological control systems have fuelled the inspiration for a large number of mathematical and logical models for control, automation and optimisation. The human brain represents the most sophisticated control architecture known to us and is a central motivation for several research attempts across various domains. In the present work, we introduce an algorithm for mathematical optimisation that derives its intuition from the hierarchical and distributed operations of the human motor system. The system comprises global leaders, local leaders and an effector population that adapt dynamically to attain global optimisation via a feedback mechanism coupled with the structural hierarchy. The hierarchical system operation is distributed into local control for movement and global controllers that facilitate gross motion and decision making. We present our algorithm as a variant of the classical Differential Evolution algorithm, introducing a hierarchical crossover operation. The discussed approach is tested exhaustively on standard test functions as well as the CEC 2017 benchmark. Our algorithm significantly outperforms various standard algorithms as well as their popular variants as discussed in the results.

1 Introduction

Evolutionary algorithms are classified as meta-heuristic search algorithms, where possible solution elements span the n-dimensional search space to find the global optimum solution. Over the years, natural phenomena and biological processes have laid the foundation for several algorithms for control and optimization that have highlighted their applicability in solving intricate optimization problems. For instance, at the cellular level in the E.Coli Bacterium, there is sensing and locomotion involved in seeking nourishment and avoiding harmful chemicals. These behavioral characteristics fuelled the inspiration for the Bacterial Foraging Optimization algorithm (Passino, 2002)(Onwubolu and Babu, 2013). Particle Swarm Optimization (Kennedy and Eberhart, 1995) is a swarm intelligence algorithm based on behavior of birds and fishes that models these particles as they traverse an n-dimensional search space and share information in order to obtain global optimum. From a biological control point, the human brain represents one of the most advanced architectures and several research attempts seek to mimic its functional accuracy, precision and efficiency. The brain function activities can be broadly classified into 2 categories: sensory and motor operations. Sensory cortical functions inspired the concept of neural networks that are being scaled successfully in deep learning to solve vast amount of problems.

The human motor function represents a distributed neural and hierarchical control system. It can be classified as having local control functions for movement as well as higher level controllers for gross motion and decision making. The execution of motor operation involves distributed brain structures at different levels of hierarchy. These include the pre-frontal cortex, motor cortex, spinal cord, anterior horn cells etc (Shaw et al., 1982). For executing an action sequence, a sequence of actions is implemented by a

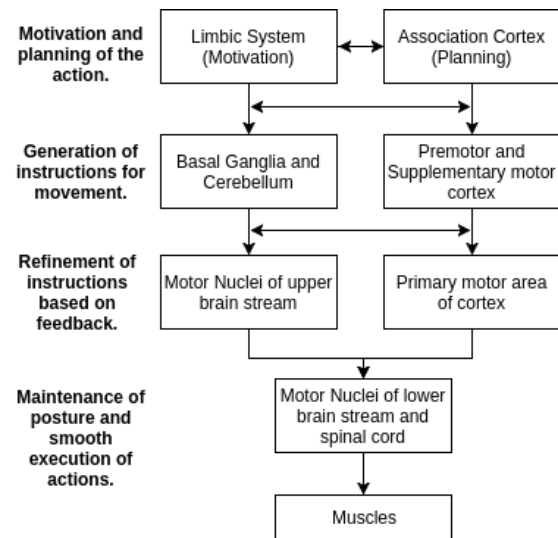


Figure 1: Hierarchy of Motor Control in Humans

string of subsequences of actions each implemented in a different part of the body. The operational structure has been depicted in Figure 1(Passino, 2005). For optimality of actions, neurons act in unison. The neurons in the motor cortex act like global leaders and send inhibitory or facilitatory influence over anterior horn cells, the local leaders, located in the spinal cord(Shaw et al., 1982). These local leaders are connected to muscle fibers, the effectors, through a peripheral nerve and neuromuscular junction. Efficient execution of task requires feedback based facilitation and inhibition of the effectors over the anterior horn cells. These sequence of operations realise the optimal convergence of the system leading to smooth motor execution.

The present work introduces an algorithm modelled intuitively on the distributed and hierarchical operation of the brain motor function.

The Classical DE Algorithm (Storn and Price, 1995), proposed by Storn and Price has been hailed as one of the premier evolutionary algorithms, owing to its simple yet effective structure(Das and Suganthan, 2011). However, in recent times, it has been criticized for its slow convergence rate and inability to effectively optimize multimodal composite functions(Das and Suganthan, 2011). This work focusses on supplementing the algorithm's performance through the introduction of hierarchical influence in the pipeline. The architecture enables the algorithm to control the flow of agents through the cumulative effect of global and local leaders in the hierarchy. The proposed approach, Hierarchy Influenced Differential Evolution (HIDE), has been subjected to exhaustive analysis on the hybrid and composite objective functions of the CEC 2017 benchmark(Awad et al., 2016). Comparison with the classical DE algorithm and its other popular variants including JADE and PSODE (Zhang and Sanderson, 2009) highlights the particular viability of the schemed approach in solving complex optimization tasks. We show that even with fixed parameters, HIDE is able to outperform adaptive architectures such as JADE by a respectable margin, as discussed in the result sections.

2 Classical Differential Evolution

The classical Differential Evolution (DE) algorithm is a population-based global optimization algorithm, utilizing a crossover and mutation approach to generate new individuals in the population for achieving optimum solutions(Das and Suganthan, 2011). For each individual x_i that belongs to the population for generation G , DE randomly samples three individ-

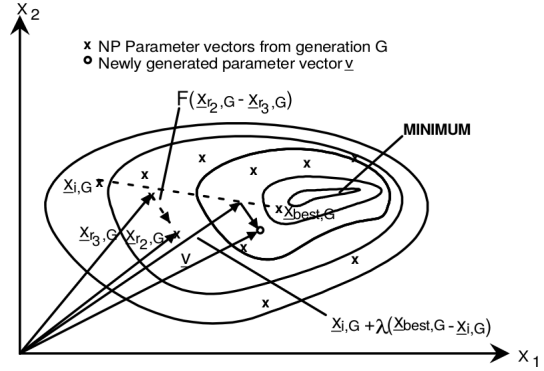


Figure 2: Motion planning of individuals in DE on two-dimensional example of objective function.

uals from the population namely $x_{r1,G}$, $x_{r2,G}$ and $x_{r3,G}$. Employing these randomly chosen points, a new individual trial vector, v_i , is generated using equation (1):

$$v_i = x_{r1,G} + F(x_{r2,G} - x_{r3,G}) \quad (1)$$

Where, F is called the differential weight (Usually lies between $[0, 1]$).

To obtain the updated position of the individual, a crossover operation is implemented between $x_{i,G}$ and v_i , controlled by the parameter CR called the crossover probability. The value for CR always lies between $[0, 1]$.

3 Hierarchy Influenced Differential Evolution

Taking inspiration from the human motor system, we model the hierarchical motor operations in our optimization agents, where we define a global leader which influences the action of several distributed local leaders and the particle agents which act as the effectors. The global leader is analogous to the decision making and planning section in the motor system hierarchy whilst, the local leaders correspond to motion generators acting under the influence of the global leader.

The position of each particle in the population is affected by the influence of global leader and local leaders, while also being affected by a randomly chosen particle from the population to induce some stochasticity in the optimization pipeline. We first model the influence of the global leader on the local leaders and the influences of the local leaders on each population element using equation (3) and (4). We introduce a hierarchical crossover between the two influencing equations governed by a hierarchical crossover parameter HC .

Analogously to the brain motor operation as depicted in Figure 1, the update of particle positions requires generating feedback for the leaders as a part of the optimization procedure, and hence the local leaders and the global leader are updated based on their objective function value generated from the perturbations in population particles. This series of events comprise of one optimization pass (one generation step). On execution of several optimization passes as described, the system is able to converge to an optimal configuration, analogous to the successful execution of the required task as shown in the final steps of Figure 1.

For each particle $x_{i,G}$, $i = 0, 1, 2, \dots, NP - 1$ for generation G , the trial vector x'_i of the particle, is governed by the hierarchical crossover operation and a mutation operation as follows :

Algorithm 1 Hierarchy Influenced Differential Evolution

```

1: procedure START
2:   Initialize parameters ( $HC, F, P, N_l, NP$ ).
3:   Generate initial global leader  $g_L$  as a random point.
4:   Generate  $N_l$  local leader points around  $g_L$  global leader.
5:   Generate  $NP$  points for population  $P$  around the local leaders using a Normal distribution with identity covariance.
6:   while Termination criteria is not met do
7:     for each individual  $x_{i,G}$  in  $P$  do
8:       Determine the corresponding local leader  $x_{L_i,G}$  from the set of all local leader based on nearest position.
9:       Let  $u = 0$  be an empty vector.
10:      Let  $G$  and  $G_t$  be the current generation and total generations of the procedure.
11:      if  $G < (HC * G_t)$  then
12:         $u_i = E_g$  from (3).
13:      else
14:         $u_i = E_l$  from (4).
15:      end if
16:       $x'_i = \text{BinomialCrossover}(u_i, x_{i,G}, CR)$ 
17:      if  $f(x'_i) < f(x_{i,G})$  then
18:        Replace  $x_{i,G}$  with  $x'_i$  in the next generation.
19:      end if
20:    end for
21:    Alter local leaders in each population cluster based on objective function value.
22:    Compute updated global leader  $g_L$ .
23:  end while
24: end procedure

```

$$u_i = \begin{cases} E_g, & \text{if } G < HC * G_t \\ E_l, & \text{otherwise} \end{cases} \quad (2)$$

$$E_g = g_L + F(x_{L_i,G} - x_{r,G}) \quad (3)$$

$$E_l = x_{L_i,G} + F(x_{i,G} - x_{r,G}) \quad (4)$$

for each dimension j of $x_{j,i,G}$:

$$x'_{j,i} = \begin{cases} x_{j,i,G} & \text{if } \text{rand}(0, 1) < HC \\ u_{j,i} & \text{otherwise} \end{cases} \quad (5)$$

$$x_{i,G+1} = \begin{cases} x'_{i,G}, & \text{if } f(x'_{i,G}) < f(x_{i,G}) \\ x_{i,G}, & \text{otherwise} \end{cases} \quad (6)$$

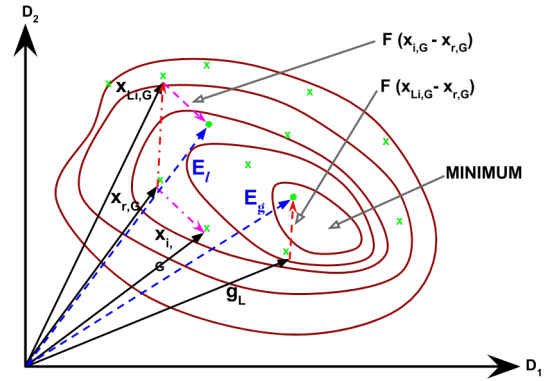


Figure 3: Hierarchical Decisive Motion planning of individuals in HIDE on two dimensional example of objective function. The position vectors resulting from the influence of global leader and local leaders are both represented as E_g and E_l on the contour of a two dimensional objective function.

Algorithm 2 Binomial_Crossover(u, x, CR)

```

1: procedure START
2:   Let  $x' = 0$  be an empty vector.
3:   Select a random integer  $k = \text{irand}(\{1, 2, \dots, d\})$ ;
   where  $d$  = number of dimensions
4:   for each dimension  $j$  do
5:     if  $\text{random}(0, 1) < CR$  or  $j == k$  then
6:       Set  $x'_j = u_j$ 
7:     else
8:       Set  $x'_j = x_j$ 
9:     end if
10:  end for
11: end procedure

```

where,

G_t is the total number of generations,
 $x_{i,G+1}$ is the vector position of $x_{i,G}$ for next generation
 F is factor responsible for amplification of differential variation,
 f is the objective function,
 $x_{i,G}$ is the current position of the individual for generation G ,
 u_i is the intermediate trial vector of the current individual,
 E_g represents the global and local leader interaction,
 E_l represents the local leader and effector interaction,
 g_L is the global leader for generation G ,
 $x_{L_i,G}$ is the position of the local leader for current individual,
 $x_{r,G} \in P$; $r \in [0,1,\dots, NP-1]$
 $x'_{j,i}$ is the trial vector

$x_{r,G}$ is randomly chosen particle from the population to induce stochasticity. The hierarchical operation is affected by the global leader g_L and the local leader $x_{L_i,G}$ through the parametric equations (3) and (4). Switching between the two is governed by the hierarchical crossover parameter HC .

3.1 Hierarchical Crossover

Convergence trend in HIDE is largely pivoted about (3) and (4), which in unison, lend a hierarchical structure to the algorithm. A successful optimization algorithm involves establishing a trade-off between exploration and exploitation. Achieving global optimization can be visualized as collaboration of two forces, exploration over a larger subspace followed by intensive exploitation over the resulting search space governed by clusters. Phase 1, involving (3) is marked by the interaction between the global and local leaders representing decision planning and facilitation of gross motion. This is followed by phase 2, involving (4) wherein the local leaders interact with and guide their effector population to control intricate motion over the constraint subspace to achieve smooth convergence. Robust convergence necessitates an optimal transition from phase 1 to phase 2 in the hierarchy. This hierarchical transition is characterized by our proposed parameter, HC . The value of HC belongs to $[0,1]$. An optimal value for HC was observed experimentally to lie about one-quarter. For the purpose of our experiments, we have fixed HC to be 0.27. Thus, this defines a deterministic cut after 27% of the total generation budget. The crossover probability defined here was observed to be mostly 50% smaller in comparison to other DE variants.

The HIDE algorithm achieves a performance im-

provement in the early optimization phase ($G < HC * G_t$) by replacing clusters of the initially generated candidate solutions with the locally best. This strategy rules out a number of mutation vectors that are more unfavorable in terms of performance gain. Additionally, by focusing on mutants of the globally best candidate solution the search space is explored rather quickly during this phase. After the population advances to $HC * G_t$ generations, the algorithm changes its reference point (the trial vector) to the locally best candidate solutions of a certain cluster. That is, having approached a closer distance from the optimal, the algorithm is able to exploit the search space. Our proposition is complemented by the observations in our results section wherein we significantly outperform several popular algorithms on involved multimodal hybrid and composite functions in higher dimensions.

4 Results and Discussions

All evaluations were performed using Python 2.7.12 with Scipy(Oliphant, 2007) and Numpy(Van Der Walt et al., 2011) for numerical computations and Matplotlib (Hunter, 2007) package for graphical representation of the result data. This section is divided into two sub-sections: Section A provides description about the problem set used for analysis of algorithmic efficiency and accuracy, and section B comprises of tabular and graphical data to reinforce the claim of superiority of the proposed approach.

Table 1: Algorithm Parameter Settings used for comparison

Algorithm	Parameter	Value
DE	F	0.5
	CR	0.9
PSODE	w	0.7298
	ϕ_p	1.49618
	ϕ_g	1.49618
	F	$r \in [0.9, 1.0)$
	CR	$r \in [0.95, 1.0)$
JADE	p	0.05
	c	0.1
HIDE	HC	0.27
	F	0.48
	CR	0.9
	N_l	5

Table 2: Objective Function Value for Dimension: 10

ID	DE		JADE		PSO-DE		HIDE	
	best	mean	best	mean	best	mean	best	mean
f_1	100.000051	100.011085	100.0	100.0	100.000712	185.975885	100.0	100.0
f_2	200.0	200.1	200.0	200.0	200.0	200.0	200.0	200.0
f_3	300.00134	300.214502	300.0	300.0	300.000006	300.000985	300.0	300.0
f_4	400.042617	403.674837	400.0	400.409399	400.064644	404.307763	400.0	400.000003
f_5	566.661791	604.867489	523.908977	541.521084	525.868824	575.61616	533.803201	579.483815
f_6	621.914237	634.807962	620.878276	636.034759	603.187964	635.865001	613.730565	629.293758
f_7	724.831278	739.129935	717.016542	723.983312	725.44788	733.15638	720.345706	725.233785
f_8	818.904202	829.749207	821.914433	826.321588	820.8941	830.246691	821.064763	828.160987
f_9	900.0	908.104383	900.0	1084.47825	900.0	1124.102561	900.0	903.454324
f_{10}	1911.51009	2447.44375	1760.95686	2162.64858	2049.64472	2518.24109	1694.43759	2049.07426
f_{11}	1102.98570	1113.42310	1105.66167	1117.50974	1105.97013	1120.19297	1101.76974	1108.86359
f_{12}	2531.74630	6509.74307	1438.60571	5430.67468	4089.00635	10810.3876	1308.43834	1327.40588
f_{13}	1313.13022	1404.90360	1304.68156	1328.75526	1319.83919	1453.34078	1306.68204	1344.28224
f_{14}	1409.94961	1426.57193	1412.93443	1428.16943	1420.91065	1434.11288	1404.92899	1410.00077
f_{15}	1504.13139	1521.44661	1502.49618	1508.31154	1501.38951	1518.31035	1500.08137	1503.16926
f_{16}	1958.42062	2104.55573	1958.85799	2094.63082	1958.41153	2048.15688	1958.43351	2062.38595
f_{17}	1728.19497	1743.15524	1730.71532	1748.12987	1727.80039	1791.60774	1723.85397	1747.58908
f_{18}	1801.58601	1838.84055	1804.29854	1825.09164	1817.15464	1840.54692	1800.23551	1804.01430
f_{19}	1901.19548	1903.60476	1900.39977	1902.15296	1902.71174	1906.25233	1900.00563	1901.01412
f_{20}	2204.55412	2289.22658	2148.53894	2178.31317	2140.56131	2261.03877	2139.91553	2172.81652
f_{21}	2337.77299	2387.23036	2314.42114	2338.68872	2337.20734	2351.89886	2320.49621	2344.61612
f_{22}	2300.80585	2304.13288	2300.0	2300.09348	2300.68418	2301.71048	2300.00002	2301.09598
f_{23}	3070.17708	3145.77229	3003.67856	3091.22041	2773.37286	3060.02252	2867.02004	3047.98231
f_{24}	2500.0	2500.0	2500.0	2500.0	2500.0	2500.0	2500.0	2500.0
f_{25}	2899.58497	2933.24981	2899.58497	2930.26651	2897.74287	2921.27479	2897.83339	2927.97651
f_{26}	2800.0	4117.597033	2800.0	2956.06417	2800.0	3367.60765	2800.0	3161.54808
f_{27}	3113.15765	3358.80643	3072.43902	3178.50964	3078.87313	3240.50181	3071.20357	3107.26854
f_{28}	3184.75565	3230.92142	3184.75565	3195.11304	3184.75565	3198.37069	3100.0	3195.41196
f_{29}	3148.58712	3266.97978	3172.40019	3233.70768	3191.34819	3244.89264	3189.21142	3292.42047
f_{30}	3442.55509	11927.40468	3207.76694	4615.59132	4573.35851	16415.1629	3205.74095	3249.71098
w/t/l	2/4/24	1/1/28	5/7/18	9/4/17	4/4/22	2/2/26	12/7/11	14/4/12

Table 3: Objective Function Value for Dimension: 30

f_{id}	DE		JADE		PSO-DE		HIDE	
	best	mean	best	mean	best	mean	best	mean
f_1	100.001508	4334.43848	100.001338	100.056201	364.295574	4236.36321	100.0	100.0
f_2	40412441.0	5.1296e+19	200.0	1535352368	332899.0	9.59068e+11	200.0	159855.5
f_3	17926.8728	22131.5427	69304.9261	74080.7004	15792.5475	21683.2090	3679.81159	8999.94726
f_4	481.255055	519.422652	403.633939	442.206911	468.341175	479.341966	400.004163	443.016156
f_5	689.041352	737.79326	667.50756	735.204027	715.904429	746.548906	685.40454	738.842184
f_6	643.626307	652.582714	651.39169	655.142819	642.724237	655.106996	644.701241	652.002395
f_7	883.347367	962.591129	779.907693	818.344111	790.014281	854.285524	812.923573	856.90477
f_8	923.37426	967.251501	931.500175	957.362003	915.414882	960.486239	930.288539	964.11663
f_9	5652.48396	7878.78144	4953.05469	5146.60095	6018.41719	9042.41018	4003.11807	4734.98436
f_{10}	3596.63104	4536.98976	4012.72329	4204.18969	3934.60671	4863.74111	3793.78177	4346.74134
f_{11}	1162.40596	1184.63401	1152.74853	1174.58813	1165.14499	1189.17178	1149.74849	1171.13041
f_{12}	56679.4351	317650.613	24821.1717	58930.0902	10221.0774	161046.055	9208.28924	41947.2226
f_{13}	3002.02949	18794.8359	4276.90774	13775.8162	3871.27983	10612.2635	1664.06241	2453.60697
f_{14}	1773.18079	5502.16038	1496.21986	42868.9158	1555.45276	4029.80853	1462.92685	1504.19151
f_{15}	1860.43566	2484.68996	1688.05046	2222.67432	1651.74747	2223.06054	1611.07440	1852.66177
f_{16}	2517.43962	2827.00496	2344.19818	2621.61868	2239.24272	2664.11466	2298.04196	2691.67481
f_{17}	2321.17594	2604.52977	2062.89802	2546.99559	2107.43677	2457.34021	1820.80664	2418.72383
f_{18}	38987.2824	94156.3285	11841.6081	184888.162	62294.8532	118430.289	12578.0037	23024.1119
f_{19}	2043.46988	3010.23537	1959.71819	2156.95787	3049.52231	6840.40839	1949.27171	1987.86676
f_{20}	2625.53915	2864.83261	2706.31444	2805.60006	2619.99649	2895.10724	2753.80621	2966.03579
f_{21}	2412.08175	2504.77777	2414.52134	2456.71898	2431.74029	2478.84135	2200.0	2442.73431
f_{22}	2300.48179	5655.56932	2300.0	4157.69878	2307.72135	6811.06916	2300.00998	6795.24842
f_{23}	3050.65450	3572.96506	2772.00202	2946.74932	2764.92246	3199.87436	2883.27689	3543.83934
f_{24}	3104.62369	3290.69875	2891.55764	2965.22556	2911.63347	2983.77293	2500.0	2940.75997
f_{25}	2916.18065	2946.71175	2875.10684	2881.09138	2875.49884	2889.94367	2874.17111	2877.48490
f_{26}	4043.69140	6756.3724	2900.0	3266.51098	2800.00780	3273.12876	2900.0	3298.49053
f_{27}	3200.00585	3998.87649	3145.81035	3189.82261	3145.42523	3639.63413	3132.81628	3284.28897
f_{28}	3290.74402	3326.26398	3100.0	3131.02731	3195.48683	3225.59405	3100.0	3115.50582
f_{29}	3720.31459	4115.18580	3305.31013	3626.88755	3535.95229	3867.59306	3352.84505	3709.10237
f_{30}	3359.03076	3900.82666	3263.49653	3749.61072	3312.63502	3524.71447	3298.70464	3421.71532
w/t/l	2/0/28	0/0/30	8/2/20	11/0/19	4/0/26	1/0/29	15/2/13	17/0/13

4.1 Problem Set Description

The set of objective functions considered for testing the proposed algorithm and compare its perfor-

mance against classical DE and its variants PSODE and JADE have been taken from the CEC 2017 set of benchmark functions. Exhaustive comparisons and analysis have been depicted on dimensions D

Table 4: Objective Function Value for Dimension: 50

f_{id}	DE		JADE		PSO-DE		HIDE	
	best	mean	best	mean	best	mean	best	mean
f_1	5884574.87	367294248.5	136.072384	3708.75086	5811.21899	154233.646	106.072862	3665.41927
f_2	4.7181e+24	3.3649e+44	2635725.0	5.0237e+26	2.2121e+19	2.5445e+23	2.2799e+17	1.0072e+31
f_3	45520.9663	62237.2968	143481.793	156166.762	52308.4274	64435.2406	44613.2999	58182.8373
f_4	574.400328	801.384952	418.580378	470.113207	477.080964	574.528479	400.005049	447.775413
f_5	816.394775	843.258843	809.89948	834.13126	778.59312	831.066954	791.405194	830.218472
f_6	652.54191	655.794152	633.21788	654.893828	653.291336	658.183613	645.25633	656.060597
f_7	1109.02123	1263.03848	889.036574	944.90319	915.153525	1047.43879	989.957862	1186.2487
f_8	1139.27892	1175.8931	1118.3391	1144.60474	1092.62639	1159.03235	1100.4760	1168.5299
f_9	22196.3878	29218.7759	11958.2800	13174.6623	24753.0405	32233.9545	10251.4763	14752.7168
f_{10}	6228.49289	7289.18367	6054.70769	6833.30631	6207.79530	7055.59523	6050.43437	6609.80456
f_{11}	1170.85860	1258.51763	1202.69485	1232.20426	1206.15456	1252.93954	1156.4396	1205.2544
f_{12}	677263.079	16987989.9	74784.6159	530814.648	584300.698	3448448.79	126908.215	494471.075
f_{13}	6005.53530	16893.94992	2041.48812	4332.5945	1572.25297	4301.82960	1484.76179	7760.05613
f_{14}	38490.5323	174367.450	2466.04705	238838.470	16327.4231	67939.0002	2967.8184	26290.3161
f_{15}	2278.14122	26989.2555	13553.0418	25636.7696	3443.58734	9167.26709	1938.20040	14976.7218
f_{16}	2722.02601	3176.91690	2345.40070	2916.56101	2521.93881	3146.04527	2436.44933	2978.37746
f_{17}	2799.94977	3289.61565	2568.38357	2907.86927	2887.28110	3236.95792	2561.37030	2874.96503
f_{18}	264037.125	872072.477	36176.5867	113941.317	26965.2851	114846.121	260540.781	536454.326
f_{19}	10051.9124	20380.2571	2089.17225	7763.17234	9905.85082	16555.7569	2013.12690	3609.25896
f_{20}	2950.92319	3274.33401	3041.81309	3113.28946	2991.58929	3361.82394	2495.03177	3080.13747
f_{21}	2596.7256	2689.68836	2526.19089	2597.6771	2555.8788	2642.38159	2447.75827	2570.91101
f_{22}	9713.99324	10803.6537	10759.5967	11032.8809	8918.43626	10465.0224	8181.4460	9755.0703
f_{23}	3451.10494	4200.17442	2971.16064	3237.77866	2977.55496	3490.63975	2851.65025	3162.31362
f_{24}	3434.46502	3682.84670	3103.95517	3185.38267	3036.79960	3158.33050s	3136.92774	3284.65609
f_{25}	3141.14488	3292.30344	2931.16295	2962.47175	2931.92695	3008.89535	2931.14231	2954.76783
f_{26}	4906.13284	7989.49096	2900.0	3346.87403	2900.44189	3653.75774	2900.0	3262.66849
f_{27}	3200.01070	3792.64558	3143.03805	3184.64635	3158.17823	3397.13032	3141.01087	3176.01152
f_{28}	3300.01082	3431.57091	3240.72586	3288.25303	3263.20714	3300.25760	3243.63199	3294.37323
f_{29}	3812.47551	4605.34953	3533.94574	3956.83524	3955.32453	4364.18129	3653.67555	3966.47195
f_{30}	3673.71196	5813.17375	3916.72571	4869.08933	3730.30935	5143.07870	3346.48367	4747.88675
w/t/l	0/0/30	0/0/30	8/1/21	9/0/21	4/0/26	3/0/27	17/1/12	18/0/12

Table 5: Objective Function Value for Dimension: 100

f_{id}	DE		JADE		PSO-DE		HIDE	
	best	mean	best	mean	best	mean	best	mean
f_1	3427212e+3	1380728e+4	141.263356	13516.69893	6067123.52	29751976.5	122.398748	11708.8236
f_2	4.196e+84	1.547e+112	8.737e+74	2.543e+87	6.153e+66	3.211e+73	3.8835e+80	8.891e+114
f_3	228808.969	262699.687	312244.360	332179.290	241427.723	257462.977	220765.083	251901.109
f_4	1975.65115	2752.24606	539.386275	677.05465	777.314462	836.965399	531.169819	621.219143
f_5	1223.53650	1286.15333	1249.19503	1307.11012	1248.41013	1310.88765	1068.11742	1272.47682
f_6	651.65013	657.84974	654.70934	659.421427	656.87704	662.31841	642.33355	654.13275
f_7	1614.00386	1920.79772	1367.06653	1536.35787	1311.84975	1534.20776	1562.37977	2076.70250
f_8	1595.41873	1736.36737	1672.56784	1768.08243	1678.12726	1761.9405	1293.55211	1592.16298
f_9	59726.5146	71986.0439	28906.9090	30336.7453	63640.3313	74961.2209	23466.5750	27067.0295
f_{10}	12005.8897	14725.3483	14227.8019	15355.6218	12937.0278	14972.9507	11153.5868	13298.0921
f_{11}	7540.6179	11481.2601	40447.5486	57228.6836	3521.90152	4544.80401	5380.43205	9916.34769
f_{12}	529993877	1881773e+3	3893556.27	6415173.60	26105108.9	41876679.1	3680108.18	10059039.6
f_{13}	7943.9249	508209.562	4622.69855	8892.77599	8246.51529	12675.8455	2976.84135	11376.9863
f_{14}	72812.8233	1329183.17	132194.795	365560.881	548410.338	941547.524	234045.940	867160.306
f_{15}	2660.46578	181957.060	1799.50650	3362.50960	1899.07344	2914.44348	1976.78912	4485.4152
f_{16}	4749.25466	5847.82673	4817.48373	5632.3022	3852.7000	5228.6635	3519.49494	4796.80272
f_{17}	4397.49635	4958.41818	3842.20601	4450.17742	3790.72056	4730.99458	3582.78588	5463.21694
f_{18}	1357845.39	1938893.27	146426.273	763318.822	1004224.20	2315010.2	631040.146	1335739.59
f_{19}	2482.1701	26455.7069	2098.9496	4767.52953	2263.72515	3927.45994	2071.07706	3664.15987
f_{20}	4968.49743	5436.60405	5231.02648	5690.74899	5109.46056	5781.30083	3627.77789	5228.43066
f_{21}	3180.74665	3355.4783	2921.90012	3085.6922	2885.57408	3127.35683	2926.35039	3199.98618
f_{22}	17808.8977	19562.9866	19213.3756	20278.9290	18695.5223	20167.41374	17548.3390	19547.1512
f_{23}	4907.51964	5819.20786	3352.5569	4222.43689	3582.04355	4779.92124	3418.98320	3609.0985
f_{24}	5173.24940	5946.12042	4060.95130	4095.42951	3801.36858	4042.42685	3998.05402	4216.82489
f_{25}	4089.11891	4548.28576	3153.48541	3236.61784	3348.38226	3407.52658	3176.3038	3264.31853
f_{26}	8557.49856	20159.1145	2900.07737	11924.79947	3021.13602	8682.03543	2900.00038	7867.5518
f_{27}	3200.02335	3772.40915	3194.80921	3201.67073	3200.02417	3494.61813	3200.02354	3200.02395
f_{28}	4947.74515	5948.21315	3295.12291	3340.28038	3456.82843	3542.57130	3300.80769	3354.71733
f_{29}	6004.77442	7090.64254	5208.71172	5970.62868	5462.32863	6178.55906	4541.19547	5739.29154
f_{30}	7798.10621	202435555	3584.97477	10674.2173	3920.32703	7139.46072	3850.31709	15318.5546
w/t/l	0/0/30	0/0/30	8/0/22	8/0/22	5/0/25	6/0/24	17/0/13	16/0/14

= 10, 30, 50 and 100 for a clear understanding of the strengths of the proposed algorithm. Objective functions $f_1 - f_3$ are simple unimodal functions and $f_4 - f_{10}$ are multimodal functions with a high num-

ber of local optima values. Functions $f_{11} - f_{20}$ are all hybrid functions using a combination of functions from $f_1 - f_{10}$. The set of composite function range from $f_{21} - f_{30}$ and merges the properties of the sub-

functions better while incorporating the basic functions as well as hybrid functions to increase complexity while maintaining continuity around the global optima.

Summarized in Table 1 are the 30 objective functions from the CEC 2017 dataset and the global optimum value for each function denoted by F^* . In all simulation runs, we set the population size NP to a fixed value of 100, and the results are shown in a tabular structure depicting the best and average values of the population individuals for the simulations. Additionally, several graphical results have been discussed to observe the convergence rate and efficiency of the algorithms used in the simulation. These graphs were plotted based on the numerical results obtained from the simulation runs used to build the tables.

4.2 Parameter Settings

The work seeks to allow transparency in results by establishing a base for fair and clear comparisons in the analysis of the algorithms. The fixed values for the parameters have been depicted in table 1. The value of F and CR have been set as 0.5 and 0.9 for DE across all experiments, as recommended in the original document in (Storn and Price, 1995), (Mezura-Montes et al., 2006), (Brest et al., 2006). The parameters for JADE were selected as suggested in the initial work (Zhang and Sanderson, 2009). The values of parameters for PSO-DE have been retained from (Liu et al., 2010) as it is one of the more cited and prestigious works. Also, we utilize the same parameter definitions for PSO as cited in this article by the initial authors in (Poli et al., 2007). The population size for initialised to 100 for all the algorithms as it is the uniformly recommended value by all of these papers. A total of 100 independent iterations were performed to obtain consistent result values to permit a uniform examination of the algorithm behaviour.

4.3 Numerical and Graphical Results

In tables 3-6, the best and mean values obtained for the population agents in the simulation runs have been reported, and the optimum values for each objective function have been highlighted in **bold**. For the sake of clarity, the comparison results in each table have been summarized in " $w/t/l$ " format wherein w represents the number of objective functions where the algorithm outperforms all other algorithms, t specifies the number of objective functions where it is tied as the best algorithm for the objective function and l represents the number of test functions where it does not finish first. The utilization of the evaluation met-

ric facilitates a definitive comparison of the different algorithms under consideration.

Tables 3 and 4 highlight the performance of the algorithms for $D = 10$ and $D = 30$ respectively. For $D = 10$, HIDE depicts impressive performance. It registered a " $w/t/l$ " score of 12/7/11 in the best case and 14/4/12 in the mean of population case. In both these test functions, JADE achieved the second best performance registering a $w/t/l$ of 5/7/18 on the best optimal value case and 9/4/17 on the mean of optimal value case. On $D = 30$, HIDE achieved maximum number of wins in both best and mean case (17 and 18 respectively). JADE achieved second position with 8 and 9 wins in the best and mean case. The decent performance of JADE can be attributed to the adaptive nature of its parameter selection which enables enhancement of its convergence rate.

The results for $D = 50$ and $D = 100$ (higher dimensions) have been summarized in tables 5 and 6. On $D = 50$, HIDE depicted exceptional performance, outperforming all other algorithms. It registered 17 wins in the best case and 18 wins in the mean case. Classical DE shows no wins in any case in high dimensional settings owing to its slow convergence rate and inability to attain global optimum thus highlighting the usefulness of the modifications introduced in the variants including HIDE. Similarly for $D = 100$, HIDE again outperforms all other algorithms by an appreciable margin. From a functional standpoint, It would be worthwhile to highlight that HIDE outperformed the other 3 compared algorithms on majority on the composite and hybrid functions, particularly on the higher dimensional settings. The efficiency of HIDE can be attributed to the hierarchical nature of crossover selection and concurrency in vector configurations at the higher hierarchy levels. The tabular results reinforce the fact that HIDE outperforms JADE, PODE and DE. On close analysis, it can be witnessed that HIDE falls behind the other algorithms on a small fraction of unimodal functions such as f_5, f_7 on lower dimensions due to fast convergence during early stages of execution. However, the performance of higher dimensions, particularly on the more involved functions highlights utility for real world problems.

The tabular results are complemented through the graphical representations in Figure 4. For the sake of clarity, representations of higher dimensional problems span more number of iterations than those for lower dimensional settings. Analysis of the plots clearly depicts that HIDE shows better convergence rate as compared to other algorithms. As the analysis transcends to higher dimensional settings, the proposed approach outperforms the other algorithms on

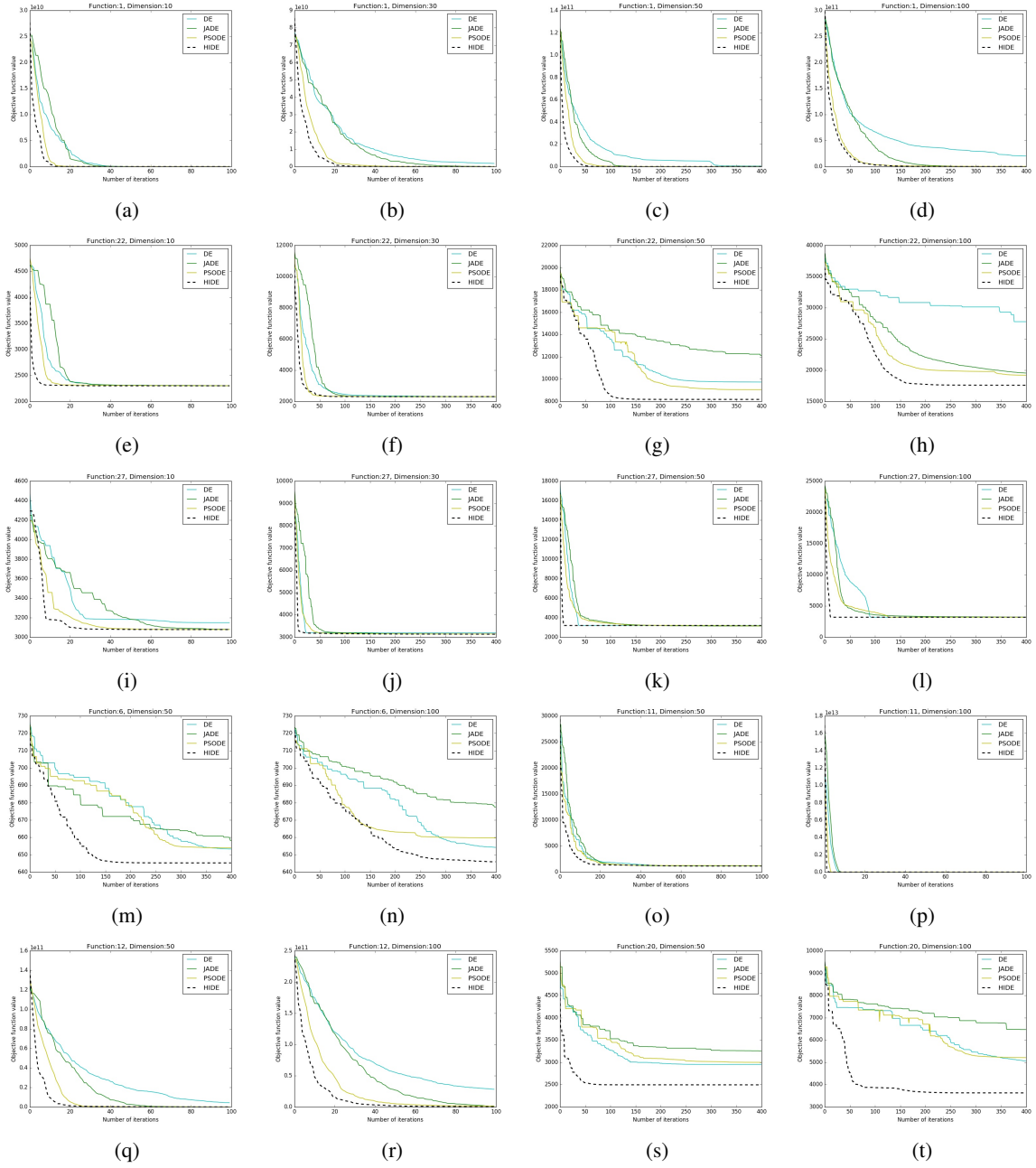


Figure 4: Comparative convergence profiles for test functions from CEC 2017 Benchmark over $D = 10, 30, 50, 100$

majority of the objective functions with respect to both convergence rate and optimality. the superiority of our algorithm in higher dimensions (50 and 100) is clearly evident from Figure 4. (m,n,q,r,s,t). Figure 4. (e,f,g,h) depict that for functions where HIDE and the other variants may depict similar trends on lower dimensions, HIDE eventually excels and surpasses them in higher dimensions in most scenarios. Almost all figures are representative of a faster convergence rate for HIDE on higher dimensions. This remarkable

trait in HIDE enhances its utility for high dimensional problems where fast convergence to global optimum value is required, hence making it superior to the other considered algorithms and several variants of the DE algorithm.

5 Conclusion

Differential Evolution has been regarded as one of the most successful optimization algorithms and over the years, several variants have been proposed to enhance its convergence rate and performance. In the present work, we introduced a hierarchy influenced variant of the classical DE algorithm and modeled the same on the brain motor operation. The algorithm was characterized by global leader, local leaders and an effector population. The global leader and distributed local leaders interacted to facilitate gross motion via a greedy exploration strategy. The local leaders and their effectors interacted to control intricate motion for smooth convergence. A hierarchical crossover parameter was introduced to characterize the hierarchical transition between the two interactions. The influence of the vector configurations at the higher levels of hierarchy enabled the algorithm to avoid local minima in most objective functions. The same is complemented through our result observations wherein we significantly outperform several popular algorithm on complex multimodal functions in higher dimensional settings. Our proposed approach has sought to establish a viable tradeoff between fast optimization, robust convergence and low number of control parameters. The performance analysis of the algorithm highlights the particular effectiveness of the proposed approach on high dimensional hybrid and composite functions. The observed results provide sufficient motivation to extend the scope of the work to complex high dimensional real life problems including image enhancement, traveling salesman problem and flexible job-shop scheduling.

REFERENCES

- Awad, N., Ali, M., Liang, J., Qu, B., and Suganthan, P. (2016). Problem definitions and evaluation criteria for the cec 2017 special session and competition on single objective real-parameter numerical optimization. *Technical Report*.
- Brest, J., Greiner, S., Boskovic, B., Mernik, M., and Zumer, V. (2006). Self-adapting control parameters in differential evolution: A comparative study on numerical benchmark problems. *IEEE transactions on evolutionary computation*, 10(6):646–657.
- Das, S. and Suganthan, P. N. (2011). Differential evolution: A survey of the state-of-the-art. *Evolutionary Computation*, *IEEE Transactions on*, 15(99):4–31.
- Dorigo, M. and Stützle, T. (2010). Ant colony optimization: overview and recent advances. In *Handbook of metaheuristics*, pages 227–263. Springer.
- Hunter, J. D. (2007). Matplotlib: A 2d graphics environment. *Computing In Science & Engineering*, 9(3):90–95.
- Kennedy, J. and Eberhart, R. (1995). Particle swarm optimization. In *Neural Networks, 1995. Proceedings., IEEE International Conference on*, volume 4, pages 1942–1948 vol.4.
- Liu, H., Cai, Z., and Wang, Y. (2010). Hybridizing particle swarm optimization with differential evolution for constrained numerical and engineering optimization. *Appl. Soft Comput.*, 10(2):629–640.
- Mezura-Montes, E. n., Velázquez-Reyes, J., and Coello Coello, C. A. (2006). A comparative study of differential evolution variants for global optimization. In *Proceedings of the 8th Annual Conference on Genetic and Evolutionary Computation, GECCO '06*, pages 485–492, New York, NY, USA. ACM.
- Oliphant, T. E. (2007). Python for scientific computing. *Computing in Science & Engineering*, 9(3):10–20.
- Onwubolu, G. C. and Babu, B. (2013). *New optimization techniques in engineering*, volume 141. Springer.
- Passino, K. M. (2002). Biomimicry of bacterial foraging for distributed optimization and control. *IEEE control systems*, 22(3):52–67.
- Passino, K. M. (2005). *Biomimicry for optimization, control, and automation*. Springer Science & Business Media.
- Poli, R., Kennedy, J., and Blackwell, T. (2007). Particle swarm optimization – an overview.
- Shaw, D. M., Kellam, A., and Mottram, R. (1982). Brain sciences in psychiatry. In Shaw, D. M., Kellam, A., and Mottram, R., editors, *Brain Sciences in Psychiatry*. Butterworth-Heinemann.
- Storn, R. and Price, K. (1995). *Differential evolution-a simple and efficient adaptive scheme for global optimization over continuous spaces*, volume 3. ICSI Berkeley.
- Van Der Walt, S., Colbert, S. C., and Varoquaux, G. (2011). The numpy array: a structure for efficient numerical computation. *Computing in Science & Engineering*, 13(2):22–30.
- Zhang, J. and Sanderson, A. C. (2009). Jade: adaptive differential evolution with optional external archive. *IEEE Transactions on evolutionary computation*, 13(5):945–958.